

Periodic Forcing and ENSO Suppression in the Cane-Zebiak Model

AIJUN PAN^{1*}, QINYU LIU¹ and ZHENGYU LIU^{2,1}

¹Physical Oceanography Laboratory, Ocean University of China, Qingdao 266003, P.R. China

²Center for Climate Research, University of Wisconsin-Madison, WI 53706-1695, U.S.A.

(Received 22 September 2003; in revised form 3 May 2004; accepted 10 May 2004)

The effect of a periodic forcing on the intensity of El Niño-Southern Oscillation (ENSO) is studied using the Cane-Zebiak model. With a basic seasonal climate close to the present, ENSO can be suppressed by a substantially enhanced seasonal external equatorial wind, which could be induced by monsoon forcing. ENSO suppression is usually more effective for an unstable self-exciting ENSO than for a stable stochastic-exciting ENSO. In addition, ENSO also tends to be suppressed by sufficiently strong periodic forcings of longer periods. The suppression of ENSO seems to be related to the nonlinear mechanism of frequency entrainment. These conclusions are in qualitative agreement with previous studies of conceptual ENSO models, although the Cane-Zebiak model shows a much more complicated dependence of the amplitude of ENSO on periodic forcing.

Keywords:

- Period forcing,
- ENSO,
- frequency entrainment,
- Cane-Zebiak model.

1. Introduction

ENSO (El Niño and Southern Oscillation), known as the most significant interannual oscillation signal in the tropical Pacific for its great impacts on global climate variability, has been most intensively researched by scientists during the past few decades (Bjerkness, 1969; Wytki, 1975; Lau, 1981; Philander *et al.*, 1984; Zebiak and Cane, 1987; Suarez and Schopf, 1988; Neelin, 1991; McCreary and Anderson, 1991; Battisti and Sarachik, 1995). Although we have come to know much about why it oscillates on the interannual time scale and why it tends to peak at the end of the calendar year (Battisti and Hirst, 1989; Jin, 1997; Tziperman *et al.*, 1997), we still cannot tell what the ENSO intensity will be in the future, which is known to be very important for human society and the natural environment.

Recent paleo proxy records in South America (Sandweiss *et al.*, 1996; Rodbell *et al.*, 1999) seem to suggest that ENSO intensity reduced before the mid-Holocene (about 6000 yr ago), for which, until now, three explanations have been offered. One is from Clement *et al.* (1999, 2000) who, using an intermediate coupled model, suggested that the ENSO event is suppressed by solar radiation forcing in the tropical Pacific coupled ocean-atmosphere system. Another explanation is attrib-

uted to Fedorov and Philander (2000). Using linear stability analysis, they showed that the coupled instability induces the ENSO reduction. Recently, it has been proposed that the Asian monsoon may affect ENSO through the atmospheric teleconnection (Barnett *et al.*, 1989; Chung and Nigam, 1999). Wang (2000) proposed a unified oscillator model in which some ENSO events depend more on equatorial wave dynamics, some on off-equatorial wind anomalies in the far western Pacific, and others are best characterized by meridional exchanges of heat between the tropics and the subtropics. One hypothesis (Liu *et al.*, 1999, 2000) on ENSO evolution during the Holocene suggests that the weaker ENSO before the mid-Holocene was induced by an enhanced northern hemisphere monsoon. Using an idealized delayed oscillator model (Schopf and Suarez, 1988, 1990), Liu (2002) further showed that ENSO suppression appears to be a general feature of the ENSO system under external periodic forcing, including seasonal forcing, and ENSO weakens when the forcing increases. This ENSO suppression can be attributed to the mechanism of “frequency entrainment”, which was first proposed by Chang *et al.* (1994) in their study of the seasonal cycle-ENSO interaction.

Here, the effect of the periodic forcing on ENSO suppression is further studied using a coupled model of intermediate complexity—the Cane-Zebiak (CZ) model (Zebiak and Cane, 1987). This model has been used by Clement *et al.* (1999, 2000) in their study of ENSO suppression in the Holocene using realistic insolation forc-

* Corresponding author. E-mail: aijunpan@163.com

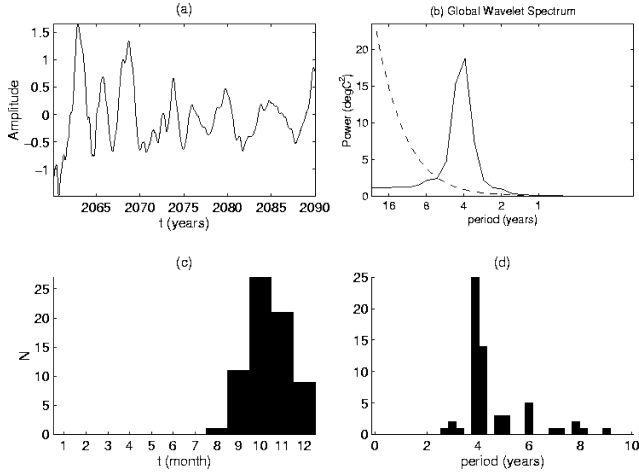


Fig. 1. Analysis of a NINO3 time series from a 500-yr standard model run ($\alpha = 1.54$, as the standard case for self-exciting unstable ENSO): (a) portion of the NINO3 time series, (b) global wavelet spectrum, dashed line is the 95% significance level, (c) a histogram of the number of ENSO events (vertical axis) per month of the calendar year, which provides a measure of the “phase locking” of ENSO, and (d) a histogram of the distribution of separation between ENSO events. Horizontal axis: separation between events in years (in a 3-month resolution); vertical axis: number of times a given separation is seen in the time series. In the histogram, an ENSO “event” is defined as a local maximum in the time series over a period of 3 years (i.e., 1.5 years before and 1.5 years after the event) with amplitude larger than the standard deviation (STD) of the NINO3 SSTA.

ing. Our contribution here is a systematic study of ENSO suppression using idealized periodic wind forcing, with an emphasis on the mechanism of ENSO suppression. In general, our study with the CZ model appears to support the simple model study of Liu (2002): the main effect of an enhanced external seasonal forcing is to reduce the amplitude of ENSO, if the forcing is realistically strong.

2. The Model

The CZ model is a perturbation model on a climatological annual cycle (Zebiak and Cane, 1987). There are five background seasonal cycle fields representing the climatologic state of the tropical Pacific ocean-atmosphere: the SST, upwelling velocity, surface winds, ocean surface currents and surface wind divergence. As the ENSO index, we here use the model’s NINO3 index (averaged sea surface temperature anomaly (SSTA) in the east Pacific 150°W – 90°W , 5°S – 5°N).

Each experiment is run for 600 yr with the last 500 yr being used for analysis. The amplitude of ENSO is defined as the standard deviations of the 12-month running mean NINO3 SSTA. The coupling parameter α rep-

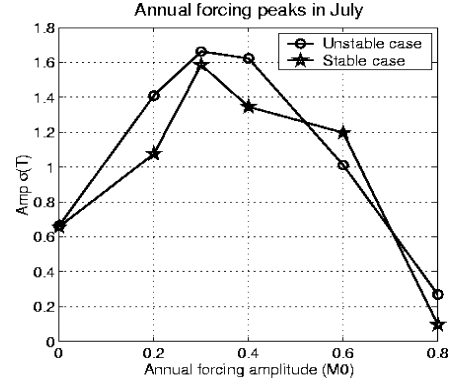


Fig. 2. Dependence of ENSO amplitude on the magnitude of anomalous monsoon wind ($M_0 = 0.2, 0.3, 0.4, 0.6, 0.8$) for both of the standard self-exciting unstable ($\alpha = 1.54$) ENSO (circle) and stochastic-exciting stable ($\alpha = 1.35$) ENSO (pentagram). The phase ϕ of the monsoon wind is specified to peak in July with $M > 0$ corresponding to an easterly anomaly and a forcing amplitude of $M_0 = 0.2$ is equivalent to a surface wind stress anomaly of 0.14 dyn cm^{-2} . Vertical axis: ENSO amplitude, Horizontal axis: amplitude of monsoon (M_0).

resents the strength of the SST-induced atmospheric heating

$$Q_s = (\alpha T) \exp\left[\frac{(T - 30^{\circ}\text{C})}{16.7^{\circ}\text{C}}\right]. \quad (1)$$

With the parameter set at 1.54 (Fig. 1), the model ENSO has an amplitude of 0.62°C and a dominant period of 4-yr, (Figs. 1(b) and (d)), with the maximum SSTA peaking around the end of the calendar year (Fig. 1(c)). These features are similar to observations. This case is the standard case for a self-exciting unstable ENSO.

We also study the case of a stable ENSO, that is, the ENSO can only sustain its interannual oscillation with a little stochastic forcing provided (Penland and Sardeshmukh, 1995). For the standard case of stable ENSO, α is chosen as 1.35, at which value the model ENSO is damped and is sustained at finite amplitude (0.62°C) with only a stochastic forcing. The characteristics of this stable ENSO are similar to the standard unstable case in Fig. 1, although the SST evolution tends to be somewhat irregular (not shown).

3. Effect of Monsoon and Other Periodic Forcing

With a stronger Asian summer monsoon, the trade winds over the eastern and central Pacific tend to be strengthened due to the anomalous Walker circulation (Barnett, 1989; Chang and Li, 2000). As a crude approximation, the monsoon effect on ENSO is simulated by imposing an annual cycle of anomalous trade winds over

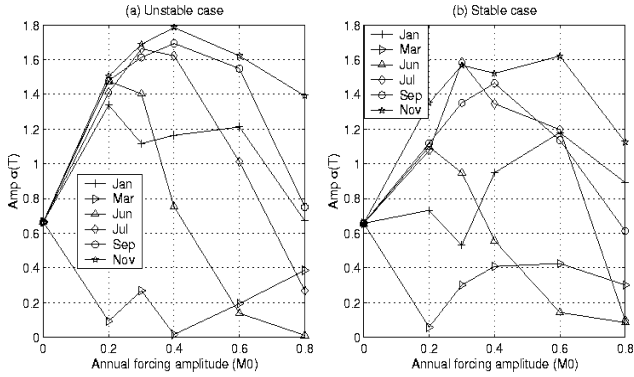


Fig. 3. Similar to Fig. 2, but as functions of the phase ϕ of the anomalous monsoon wind, which is specified to peak in January (plus), March (triangle right), June (triangle up), July (diamond), September (circle) and November (pentagram) for both the standard unstable ($\alpha = 1.54$) ENSO (a) and stable ($\alpha = 1.35$) ENSO (b), respectively.

the entire tropic Pacific Ocean. The anomalous zonal wind takes the form

$$M(t) = M_0 \sin(\omega \times t - \phi) \quad (2)$$

where ω is the annual frequency, M_0 and ϕ are the amplitude and phase of the anomalous monsoon wind, respectively. The phase ϕ is specified to peak in July with $M > 0$ corresponding to an easterly anomaly. A forcing amplitude of $M_0 = 0.2$ is equivalent to a surface wind stress anomaly of 0.14 dyn cm^{-2} . The imposed anomalous trade wind is zonally uniform, and meridionally confined between 5°S and 5°N with a Gaussian distribution. Admittedly, this is an overly simplified picture of the monsoon effect on ENSO.

This monsoon wind can also suppress ENSO for both unstable self-exciting ENSO and stable stochastic-exciting ENSO. Figure 2 shows the dependence of the ENSO amplitude on the magnitude of anomalous monsoon wind for both the standard unstable and stable ENSOs. For both ENSOs, with the strengthening of anomalous annual wind, ENSO first intensifies (until $M_0 = 0.3$) and then weakens. Therefore, qualitatively, ENSO suppression in the CZ model is similar to the delayed oscillator model (Schopf and Suarez, 1988, 1990).

The general feature of ENSO suppression of equatorial wind seems not to be very sensitive to the phase of this external wind. Figure 3 further shows the dependence of the amplitude of ENSO on the wind anomalies that peak in different months. Both an unstable ENSO (Fig. 3(a)) and a stable ENSO (Fig. 3(b)) are shown. It is seen that ENSO suppression is rather insensitive to the peak month, if the peak month in spring to fall. The in-

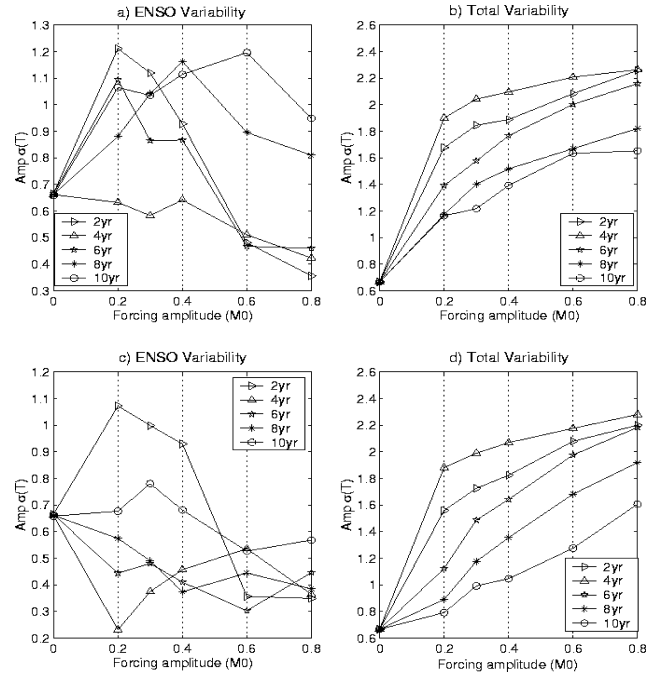


Fig. 4. Amplitude of (a) ENSO and (b) total variability as a function of the forcing period for the case of a self-exciting unstable ENSO ($\alpha = 1.54$). Five anomalous periodic winds are used: 2 yr (triangle right), 4 yr (triangle up), 6 yr (pentagram), 8 yr (star) and 10 yr (circle). (c)–(d) is the same as (a)–(b), except for the case of a stochastic-exciting stable ENSO ($\alpha = 1.35$).

sensitivity suggests that ENSO suppression is largely due to frequency entrainment, which in principle is independent of the phase of the forcing. However, if the peak month lies in winter to spring (especially March), ENSO suppression becomes stronger. This dependence of ENSO suppression on the phase of forcing is somewhat different from the simple model study (Liu, 2002), which shows little sensitivity of ENSO suppression to the peak month of the external wind. This difference is partly due to differences in the expressed form of the background seasonal cycle. In the delayed oscillator model the periodic forcing wind can only change the nonlinear term and constant term in model equation (see equation (4) in Liu (2002)), while the coefficient of the main term is not changed when the phase of this external wind forcing is changed. But, in the CZ model, the phase of periodic external wind can control the background surface wind, current and upwelling, which can in turn affect the phase of ENSO.

More quantitatively, however, ENSO suppression starts when the anomalous wind is stronger than about $M_0 = 0.3$ for anomalous wind peaking in summer, corresponding to an anomalous wind (0.2 dyn cm^{-2}), which is about 40% of the mean trade wind stress.

Finally, as in Liu (2002), we also studied the effect of external wind forcing with different periods. Figure 4 shows the dependence of ENSO amplitude on the external wind with periods of 2 yr, 4 yr, 6 yr, 8 yr and 10 yr, for the unstable (Fig. 4(a)) and stable (Fig. 4(c)) ENSO. In Figs. 4(a) and (c) the amplitude of ENSO is now calculated using the residual SST, in which the variation of the SST with forcing periods is subtracted (total variation of SST anomaly minus SST variability with the forcing periods). Overall, although the total variability (Figs. 4(b) and (d)) increases with the external forcing, ENSO variability shows a similar suppression to the annual wind (Fig. 2). Certainly, the suppression is the strongest for the 4-year periodic forcing, because when we calculate the residual SST, all variation with 4-year period was subtracted. The 4-year period is closest to the period of ENSO (Figs. 1(b) and (d)). Therefore, as in Liu's (2002) study, ENSO suppression is a general feature under a periodic forcing. The total variability (Figs. 4(b) and (d)) increases with the external forcing; most efficient suppression occurs when the forcing period (4-years) is close to natural variability, due to nonlinear resonance. This again is a confirmation that ENSO suppression occurs in the CZ model due to frequency entrainment.

4. Summary

The CZ model has been used to study the potential impact of seasonal forcing on ENSO intensity. For a basic climate comparable with the present, it is found that ENSO tends to be suppressed by a sufficiently strong monsoon. ENSO suppression seems to be caused by frequency entrainment and is robust for both of the unstable and stable ENSO. In addition, ENSO is also suppressed by an enhanced periodic forcing of interannual to decadal periods. Therefore, the response of ENSO to periodic forcing in the CZ model is qualitatively similar to the delayed oscillator model (Schopf and Suarez, 1988, 1990) and in the recharge model of Jin (1997). We do not discuss the response of ENSO to periodic forcing in the West Pacific oscillator model (Wang and Weisberg, 1998) and the unified oscillator model (Wang, 2000). Similar features may exist, because the main physical processes are same in the conceptually different models.

The CZ model overcomes one of the most serious problems of the idealized delayed oscillator model: the uncertainty of the parameter regime associated with the realistic mean climatology. Our study with the CZ model represents a major step forward from the delayed oscillator model, because the former has a much more realistic mean climate as well as variability. Our results using the CZ model therefore suggest that the effect of the seasonal forcing on ENSO could occur in a realistic climate state and therefore is of practical importance for the interpretation of observations. For an anomalous trade wind,

which is likely to be induced by an anomalous monsoon wind, ENSO suppression does not occur until the anomalous wind is stronger than about 0.2 dyn cm^{-2} . This is a dramatic change of the trade wind, although not impossible in the real world. This quantitative conclusion, however, remains to be further clarified. First of all, our anomalous trade wind is extremely idealized. Second, part of the monsoon effect is already built into the background seasonal cycle. It is unclear yet how the external monsoon effect can be combined with the prescribed annual cycle field to represent the increased monsoon effect.

Since the CZ model demonstrates the possibility of ENSO intensity changes due to the change of the periodic forcing for realistic climates, the concept of ENSO suppression could potentially be useful for the interpretation of the observed variation of ENSO in the real world. One important potential application is the interaction between monsoon and ENSO. Previous studies showed complex and inconclusive two-way interactions between the Asian monsoon and ENSO in the CZ model (Chung and Nigam, 1999). Here, our study shows that, even with the one-way seasonal forcing of ENSO, the intensity of ENSO shows complex changes, much more complicated than in an idealized delayed oscillator model. Therefore, further studies are much needed for a better understanding of the impact of seasonal forcing on ENSO, as well as the feedback of ENSO on seasonal variability, such as the Asian monsoon.

Acknowledgements

This work is supported by Chinese NSFC (No. 40028605 and No. 40233033). Also, great thanks are given to the two reviewers for their excellent and admirable suggestions.

References

- Barnett, T. P. *et al.* (1989): The effect of Eurasian snow cover on regional and global climate variations. *J. Atmos. Sci.*, **48**, 661–685.
- Battisti, D. S. and A. C. Hirst (1989): Interannual variability in a tropical atmosphere-ocean model: influence of the basic state, ocean geometry and nonlinearity. *J. Atmos. Sci.*, **46**, 1687–1708.
- Battisti, D. S. and E. S. Sarachik (1995): Understanding and predicting ENSO. *J. Geophys. Res.*, **33**, Suppl., 1367–1376.
- Bjerkness, J. (1969): Atmospheric teleconnection from equatorial Pacific. *Mon. Wea. Rev.*, **97**, 163.
- Chang, C.-P. and T. Li (2000): A theory for the tropospheric biennial oscillation. *J. Atmos. Sci.*, **57**, 2209–2224.
- Chang, P., B. Wang, T. Li and L. Ji (1994): Interactions between the seasonal cycle and the southern oscillation—frequency entrainment and chaos in a coupled ocean-atmosphere model. *Geophys. Res. Lett.*, **21**, 2817–2820.
- Chung, C. and S. Nigam (1999): Asian summer monsoon-ENSO feedback on the Cane-Zebiak model. *J. Climate*, **12**, 2782–2807.

- Clement, A. C., R. Seager and M. A. Cane (1999): Orbital controls on ENSO and tropical climate. *Paleoceanography*, **14**, 441–456.
- Clement, A. C., R. Seager and M. A. Cane (2000): Suppression of El Niño during the mid-Holocene by changes in the Earth's orbit. *Paleoceanography*, **15**, 731–737.
- Fedorov, A. and G. Philander (2000): Is El Niño changing? *Science*, **288**, 1997–2002.
- Jin, F. F. (1997): An equatorial ocean recharge paradigm for ENSO. Part I: Conceptual model. *J. Atmos. Sci.*, **54**, 811–847.
- Lau, K. M. (1981): Oscillations in a simple equatorial climate system. *J. Atmos. Sci.*, **38**, 248–261.
- Liu, Z. (2002): A simple model study of ENSO suppression by external periodic forcing. *J. Climate*, **15**, 1088–1098.
- Liu, Z., R. Jacobs, J. Kutzbach, S. Harrison and J. Anderson (1999): Monsoon impact on El Niño variability in the early Holocene. *PAGE Newsletter*, **7**, No. 2, 16–17.
- Liu, Z., J. Kutzbach and L. Wu (2000): Modeling climatic shift of El Niño variability in the Holocene. *Geophys. Res. Lett.*, **27**(15), 2265–2268.
- McCreary, J. P. and D. Anderson (1991): An overview of coupled ocean-atmosphere models of El Niño and the Southern Oscillation. *J. Geophys. Res.*, **96**, Suppl., 3125–3150.
- Neelin, J. D. (1991): The slow sea surface temperature mode and the fast-wave limit: analytic theory for tropical interannual oscillations and experiments in a hybrid-coupled model. *J. Atmos. Sci.*, **48**, 584–606.
- Penland, C. and P. Sardeshmukh (1995): The optimal growth of the tropical sea surface temperature anomalies. *J. Climate*, **8**, 1999–2024.
- Philander, S. G. H., T. Yamagata and R. C. Pacanowski (1984): Unstable air-sea interactions in the tropics. *J. Atmos. Sci.*, **41**, 604–613.
- Rodbell, D. T. *et al.* (1999): An ~15,000-year record of El Niño-Driven Alluviation in southwestern Ecuador. *Science*, **283**, 516–520.
- Sandweiss, D. *et al.* (1996): Geoarchaeological evidence from Peru for a 5000 years B.P. onset of El Niño. *Science*, **273**, 1531–1533.
- Schopf, P. S. and M. J. Suarez (1990): Ocean wave dynamics and the timescale of ENSO. *J. Phys. Ocean*, **20**, 629–645.
- Suarez, M. J. and P. S. Schopf (1988): A delayed action oscillator for ENSO. *J. Atmos. Sci.*, **45**, 549–566.
- Tziperman, E., S. Zebiak and M. Cane (1997): Mechanisms of seasonal-ENSO interaction. *J. Atmos. Sci.*, **54**, 61–71.
- Wang, C. (2000): On the atmospheric responses to tropical Pacific heating during the mature phase of El Niño. *J. Atmos. Sci.*, **57**, 3767–3781.
- Wang, C. and R. H. Weisberg (1998): Climate variability of the coupled tropical-extratropical ocean-atmosphere system. *Geophys. Res. Lett.*, **25**, 3979–3982.
- Wyrki, K. (1975): El Niño—The dynamic response of the equatorial Pacific Ocean to atmospheric forcing. *J. Phys. Oceanogr.*, **5**, 572–584.
- Zebiak, S. E. and M. A. Cane (1987): A model El Niño-Southern Oscillation. *Mon. Wea. Rev.*, **115**, 2262–2278.